

## Synthesis and biological evaluation of heterocycle containing adamantane 11 $\beta$ -HSD1 inhibitors

Vince S. C. Yeh,\* Jyoti R. Patel,\* Hong Yong, Ravi Kurukulasuriya, Steven Fung, Katina Monzon, William Chiou, Jiahong Wang, Deanne Stolarik, Hovis Imade, David Beno, Michael Brune, Peer Jacobson, Hing Sham and J. T. Link

Metabolic Disease Research, Abbott Laboratories, 100 Abbott Park Road, AP-10,304B, Abbott Park, IL 60064, USA

Received 30 May 2006; revised 15 July 2006; accepted 17 July 2006

Available online 8 August 2006

**Abstract**—A series of metabolically stable adamantane amide 11 $\beta$ -HSD1 inhibitors have been synthesized and biologically evaluated. These compounds exhibit excellent HSD1 potency and HSD2 selectivity and good pharmacokinetic and pharmacodynamic profiles.

© 2006 Elsevier Ltd. All rights reserved.

11 $\beta$ -Hydroxysteroid dehydrogenase type 1 (11 $\beta$ -HSD1) has attracted significant attention from the pharmaceutical research community as a target for the treatment of metabolic syndrome.<sup>1</sup> This endoplasmic reticulum-associated enzyme converts the glucocorticoid receptor (GR) inactive cortisone (dehydrocorticosterone in rodents) into the GR active hormone cortisol (corticosterone in rodents). In the liver, cortisol stimulates gluconeogenesis through upregulation of enzymes such as phosphoenolpyruvate carboxykinase and glucose 6-phosphatase, and in adipose tissue, cortisol promotes adipogenesis and lipolysis.<sup>2</sup> A related enzyme, 11 $\beta$ -HSD2, catalyzes the reverse reaction which in tissues like kidney protects the mineralocorticoid receptor from activation by cortisol.<sup>3</sup> The current hypothesis is that a small molecule therapeutic that selectively targets 11 $\beta$ -HSD1 can be a viable strategy for the treatment of metabolic syndrome.

We have identified adamantane amides exemplified by **1**<sup>4</sup> from initial hit to lead work, which are potent inhibitors of human and mouse 11 $\beta$ -HSD1 with selectivity over 11 $\beta$ -HSD2 (Fig. 1). Although **1** has an excellent in vitro activity against the targeted enzymes, it has a poor pharmacokinetic (PK) profile in mice. This is due to metabolism of the phenoxy side chain,

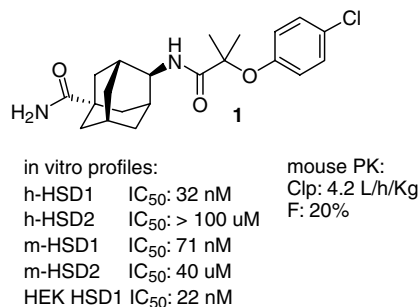


**Figure 1.** Adamantane amide 11 $\beta$ -HSD inhibitor.

as determined by in vitro mouse liver microsomal stability studies, and primary amide hydrolysis in mouse serum. The primary carboxamide on the adamantane contributes to its potent activity as well as the metabolic stability of the adamantane head group. Easily accessible secondary and tertiary adamantane carboxamide analogs were either not active or lacked acceptable PK profiles. Moreover, analogs related to **1** that contain non-polar aromatic phenoxy groups have limited metabolic stability.

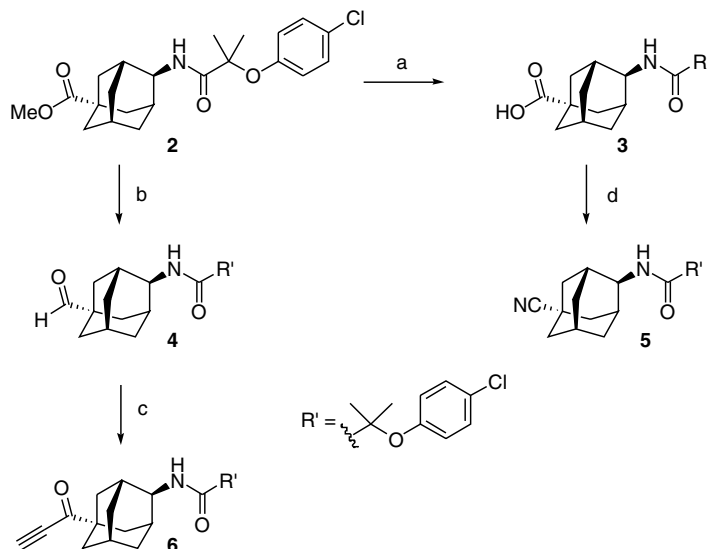
Our goal is to discover compounds that will provide long enough coverage for BID dosing for in vivo efficacy studies in rodents. Hence, desirable compounds should have a PK profile with greater bioavailability and lower clearance. We attempted to address these challenges via

**Keywords:** 11 $\beta$ -HSD1; Adamantane amide; Heterocycles; Metabolic syndrome; Metabolic stability.

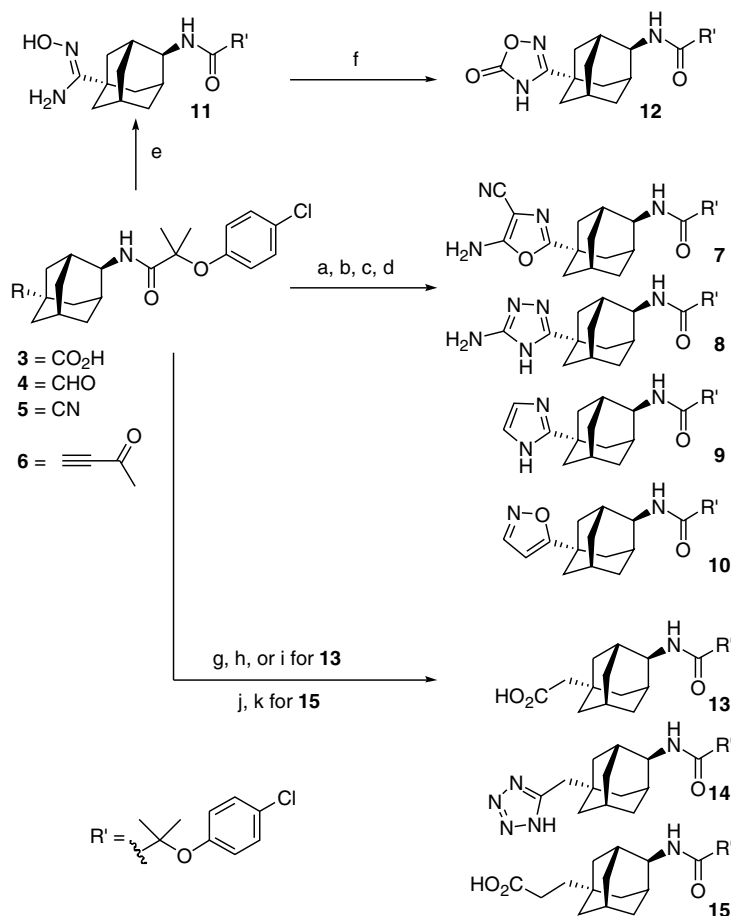
\* Corresponding authors. Fax: +1 847 938 1674; e-mail addresses: [vince.yeh@abbott.com](mailto:vince.yeh@abbott.com); [jyoti.patel@abbott.com](mailto:jyoti.patel@abbott.com)

two concerted approaches: (1) identify hydrolytically stable carboxamide bioisosteres that maintain high potency and selectivity; (2) prepare compounds contain-

ing more polar heteroaromatic side chains which exhibit metabolic stability and improvements in PK profile. In this paper, we report our initial results.



**Scheme 1.** Reagents and conditions: (a) KOTMS, THF, rt; (b) i—LiAlH<sub>4</sub>, THF, 0 °C; ii—Dess–Martin periodinane, CH<sub>2</sub>Cl<sub>2</sub>; (c) i—acetyleneMgBr, THF, 0 °C; ii—Dess–Martin periodinane, CH<sub>2</sub>Cl<sub>2</sub>; (d) i—EDCI, HOBT, *i*-Pr<sub>2</sub>NEt, then NH<sub>3</sub>; ii—TFAA, Et<sub>3</sub>N, CH<sub>2</sub>Cl<sub>2</sub>, 0 °C.



**Scheme 2.** Reagents and conditions: (a) 3, 2-amino-malononitrile, EDCI, pyr, rt; (b) i—3, aminoguanidine, EDCI, Et<sub>3</sub>N, DMF, rt; ii—tol, 100 °C; (c) 4, glyoxal, NH<sub>3</sub>, MeOH, rt; (d) 6, NH<sub>2</sub>OH, DBU, DMF, 80 °C; (e) 5, NH<sub>2</sub>OH, DBU, DMSO, 100 °C; (f) CDI, DBU, CH<sub>3</sub>CN, rt; (g) 4, TOSMIC, KOtBu, DME, MeOH; (h) ZnBr<sub>2</sub>, NaN<sub>3</sub>, H<sub>2</sub>O, 150 °C; (i) 1 N HCl, reflux; (j) 4, Ph<sub>3</sub>P=CHCO<sub>2</sub>Me, CH<sub>2</sub>Cl<sub>2</sub>; (k) i—H<sub>2</sub>, Pd/C, MeOH; ii—LiOH, MeOH/H<sub>2</sub>O.

Ester **2** was converted into compounds **3–6** using standard functional group transformations (Scheme 1). Compounds **3–6** served as starting materials for the syntheses of a number heterocycle bioisosteres of the primary amide.

Acid **3** was converted into amino oxazole **7**<sup>5</sup> and amino triazole **8** (see Scheme 2 and Table 1). Aldehyde **4** was transformed into imidazole **9**. Isoxazole **10** was derived from alkynone **6**. Addition of hydroxylamine to cyanide **5** gave hydroxyamidine **11**, which was then converted into **12**. In addition, we also explored the possibility of extending the polar group 1 or 2 carbons away from the adamantane head group. The syntheses of homologated analogs utilized either TOSMIC or stabilized Wittig reagents on aldehyde **4** (Scheme 2), followed by tetrazole synthesis (**14**) or hydrolysis to give the corresponding acids **13** and **15**.

Modification of the side chain was achieved by replacing the phenoxy group of **1** by a pyridyl group. The heteroaromatic group can either be linked through an oxygen spacer, such as **22**, or be directly attached to the quaternary carbon bearing the *gem*-dimethyl groups, such as

**27** (Table 2). The syntheses of these side chains are depicted in Schemes 3 and 4.

The *O*-linked hetroaryl analogs were prepared by nucleophilic aromatic substitution of a chloropyridine by hydroxy ester **16** followed by the attachment of adamantane **21**<sup>4</sup> and conversion to primary carboxamide (Scheme 3). Pyridyl bromide **22** was further elaborated via copper (I) catalyzed C–N coupling<sup>6</sup> to give **24–26**.

The C-linked analogs such as **28** were synthesized by a palladium catalyzed coupling<sup>7</sup> of silyl ketene acetal **19** with a pyridyl bromide such as **18** followed by acylation with adamantane **21** and conversion to the corresponding carboxamide by similar methods as those described for **22** (Scheme 4). The amino substituents of **28** and **29** were attached by nucleophilic substitution reactions.

These compounds were tested against both human and mouse 11 $\beta$ -HSD1 and 11 $\beta$ -HSD2 enzymes as well as a cell based assay with 11 $\beta$ -HSD1 overexpressed in human embryonic kidney cells (HEK).<sup>8</sup> In addition, metabolic stability of these compounds was determined using mouse liver microsomal incubation studies.

**Table 1.** In vitro inhibition and metabolic stability data for **6–14**

Compound	R	IC <sub>50</sub> <sup>a</sup> (nM)			Microsomal stability <sup>b</sup> (% remaining)
		h-HSD1/h-HSD2	m-HSD1/m-HSD2	h-HSD1 HEK	
<b>7</b>		146/>100,000	205 / 50,000	306	25
<b>8</b>		35/55,000	53/>100,000	476	41
<b>9</b>		10/11,000	11/100,000	110	3
<b>10</b>		105/15,000	71/15,000	31	30
<b>11</b>		39/100,000	26/>100,000	124	64
<b>12</b>		358/35,000	101/100,000	532	Not determined
<b>13</b>		45/52,000	92/20,700	82	94
<b>14</b>		41/>100,000	87/7,000	119	79
<b>15</b>		89/100,000	74/28,000	455	78

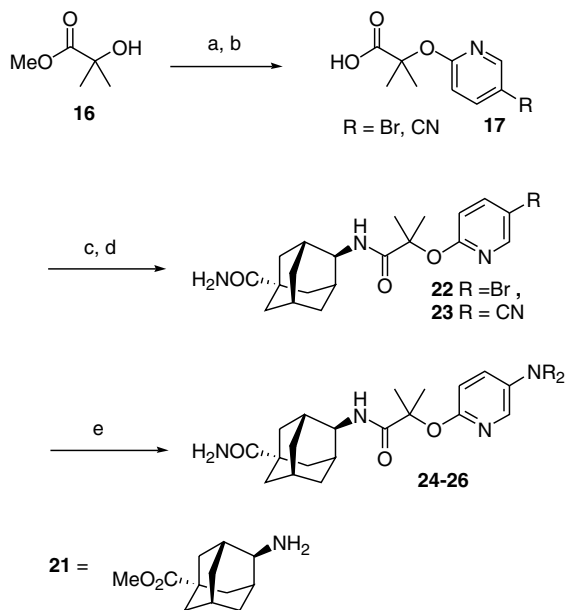
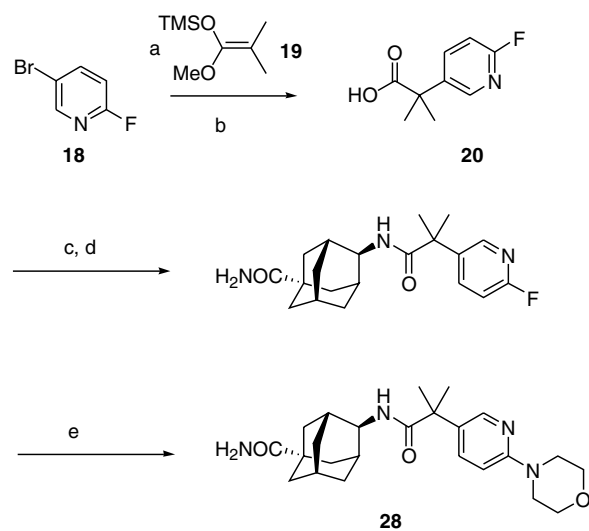
<sup>a</sup> Values are means of two experiments.

<sup>b</sup> % remaining after a 30 min incubation with mouse liver microsome.

**Table 2.** In vitro inhibition and metabolic stability data for **22–29**

Compound	X	IC <sub>50</sub> <sup>a</sup> (nM)			Microsomal stability <sup>b</sup> (% remaining)
		h-HSD1/h-HSD2	m-HSD1/m-HSD2	h-HSD1 HEK*	
<b>22</b>		6/49,000	4/>100,000	18	87
<b>23</b>		28/>100,000	36/>100,000	373	90
<b>24</b>		44/>100,000	51/>100,000	444	89
<b>25</b>		185/>100,000	519/>100,000	>10,000	ND
<b>26</b>		5/>100,000	11/>100,000	38	83
<b>27</b>		14/>100,000	65/15,000	165	100
<b>28</b>		47/>100,000	59/>100,000	169	87
<b>29</b>		29/>100,000	310/>100,000	246	83

ND, not determined as in Table 1.

<sup>a</sup> Values are means of two experiments.<sup>b</sup> % remaining after a 30 min incubation with mouse liver microsomes.**Scheme 3.** Reagents and conditions: (a) NaH, 5-bromo-2-fluoropyridine, THF/DMPU rt; (b) KOTMS, THF, rt; (c) **17**, **21**, HATU, *i*-Pr<sub>2</sub>NEt, CH<sub>2</sub>Cl<sub>2</sub>; (d) i—KOTMS, THF; ii—EDCI, HOBT, NH<sub>3</sub>, CH<sub>2</sub>Cl<sub>2</sub>; (e) **22**, morpholine, CuI, proline, K<sub>2</sub>CO<sub>3</sub>, DMSO, 120 °C.**Scheme 4.** Reagents and conditions: (a) **19**, ZnF<sub>2</sub>, Pd<sub>2</sub>(dba)<sub>3</sub>, P(*t*-Bu)<sub>3</sub>HBF<sub>4</sub>, DMA, 120 °C; (b) KOTMS, THF, rt; (c) **20**, **21**, HATU, *i*-Pr<sub>2</sub>NEt, CH<sub>2</sub>Cl<sub>2</sub>; (d) i—KOTMS, THF; ii—EDCI, HOBT, NH<sub>3</sub>, CH<sub>2</sub>Cl<sub>2</sub>; (e) morpholine, *i*-Pr<sub>2</sub>NEt, *i*-PrOH 100 °C.

Data for compounds from the adamantane head group modification are shown in Table 1. Polar heterocycles such as **8** and **9** were found to be potent and selective for the 11 $\beta$ -HSD1 enzymes. However, most of these compounds generally showed a shift in potency in the HEK assays. Currently, we do not fully understand the cause for the differences in the magnitude of potency shifts between compounds. Presumably, it is due to subtle differences in ionization of these polar groups which led to poorer cell penetration. The cellular assay was used to give us rough estimates on the ability of these compounds to inhibit 11 $\beta$ -HSD1 in vivo, therefore, potency shifts up to 10-fold were considered acceptable in this assay. A better predictor of in vivo performance is the metabolic stability assay, unfortunately, heterocycles **7–10** were rapidly metabolized in microsomal stability screen. Hydroxyamidine **11** was a potent and selective inhibitor which exhibited better metabolic stability than the above heterocyclic compounds. On the other hand, the homologated analogs **13–15** performed very well in all the in vitro assays, including remarkably improved metabolic stability.

Table 2 shows the biological results of compounds with polar heteroaromatic side chains. Several of these compounds are potent with pyrazolyl analog **26** reaching 5 nM with excellent selectivity against HSD2. Many of these compounds also possess good metabolic stability. Similar to our earlier observation in Table 1, compounds with fully basic groups at the side chain such as **25** suffered poor cellular penetration as determined by the HEK assay. In order to identify compounds suitable for in vivo efficacy studies in rodent models, selected compounds from Tables 1 and 2 were further examined in mouse ex vivo pharmacodynamic (PD)<sup>9</sup> as well as PK studies and the results are summarized in Tables 3 and 4. We were interested in compounds that exhibit robust inhibition of 11 $\beta$ -HSD1 in liver and fat tissues at extended time points (i.e., 7 and 16 h) post-dose. We hypothesize that compounds with such characteristics will allow sufficient coverage using a BID dosing regiment. The inhibition of 11 $\beta$ -HSD1 in brain has been implicated in enhancing memory and learning.<sup>10</sup> Therefore, inhibition of the target enzyme was also measured in brain tissue to help us determine the ability of these compounds to either enter or be excluded from the brain.

Hydroxyamidine **11** showed robust inhibition of 11 $\beta$ -HSD1 in liver, fat, and brain tissues through 16 h. However, it showed rapid clearance and a short half-life

Table 3. Ex vivo pharmacodynamic data<sup>a</sup>

Compound	% inhibition in liver 7 h/16 h	% inhibition in fat 7 h/16 h	% inhibition in brain 7 h/16 h
<b>11</b>	89/84	92/67	85/79
<b>13</b>	40/0	70/35	ND
<b>14</b>	62/37	17/20	11/9
<b>15</b>	99/93	50/37	67/18
<b>22</b>	57/0	47/23	ND

ND, not determined.

<sup>a</sup> See Ref. 9 for a description of the assay.

Table 4. Mouse PK data<sup>a</sup>

Compound	nAUC ( $\mu\text{g}^*\text{h/mL}$ )	CLp (L/h/Kg)	$t_{1/2}$ (h)	F (%)
<b>11</b>	1.35	4.6	0.4	61.6
<b>13</b>	46.7	0.2	2.0	96.1
<b>14</b>	3.4	1.2	2.3	39.7
<b>15</b>	11.4	0.8	2.6	86.3

<sup>a</sup> Calculated from 10 mg/kg iv and oral po dosing. Measured in plasma.

(Table 4, entry 1). This observation might be attributed to an active metabolite. The one carbon homologated acid **13** displayed long-acting PD activity in fat tissue, but shorter activity in the liver. The PK profile of **13** features low clearance, long half-life, and excellent bioavailability. Tetrazole **14** gives good inhibition of 11 $\beta$ -HSD1 in both liver and fat tissues, and it is mostly excluded from brain. The two carbon homologated acid **15** showed robust activity in fat, liver, and brain. Compound **15** is also accompanied with excellent PK data. Compound **22** showed moderate activity at 7 h (Table 3), but no activity in liver at 16 h. This might be due to extensive primary amide hydrolysis to the corresponding inactive acid at longer time points. In fat **22** shows higher activity than liver. All the compounds that we have evaluated in PK studies showed significantly improved bioavailability as compared to **1**.

In conclusion, we have identified a series of modifications to the 11 $\beta$ -HSD inhibitor **1** that resulted in improved PD and PK profiles. Efforts are currently underway to combine a favorable functional group at the adamantane head group with a polar heterocycle containing side chain that we have identified over the course of this work into one molecule. We anticipate that these hybrid molecules will have good combined PK and PD profiles in addition to other desirable properties such as increased water solubility. The results from this effort will be reported in due course.

## References and notes

- For a review on patents, see: Fotsch, C.; Askew, B. C.; Chen, J. J. *Expert Opin. Ther. Pat.* **2005**, *3*, 289; (a) Barf, T.; Vallgarda, J.; Emond, R.; Haggstrom, C.; Kurz, G.; Nygren, A.; Larwood, V.; Mosialou, E.; Axelsson, K.; Olsson, R.; Engblom, L.; Edling, N.; Ronquist-Nii, Y.; Ohman, B.; Alberts, P.; Abrahamson, L. *J. Med. Chem.* **2002**, *45*, 3813; (b) Hermanowski-Vosatka, A.; Balkovec, J. M.; Cheng, K.; Chen, H. Y.; Hernandez, M.; Koo, G. C.; Grand, C. B. L.; Li, Z.; Metzger, J. M.; Mundt, S. S.; Noonan, H.; Nunes, C. N.; Olson, S. H.; Pikounis, B.; Ren, N.; Robertson, N.; Schaeffer, J. M.; Shah, K.; Springer, M. S.; Strack, A. M.; Strowski, M.; Wu, K.; Wu, T.; Xiao, J.; Zhang, B. B.; Wright, S. D.; Thieringer, R. *J. Exp. Med.* **2005**, *202*, 517; (c) Olson, S.; Aster, S. D.; Brown, K.; Carbin, L.; Graham, D. W.; Hermanowski-Vosatka, A.; LeGrand, C. B.; Mundt, S. S.; Robbins, M. A.; Schaeffer, J. M.; Slossberg, L. H.; Szymonifka, M. J.; Thieringer, R.; Wright, S. D.; Balkovec, J. M. *Bioorg. Med. Chem. Lett.* **2005**, *15*, 4359; (d) Gu, X.; Dragovic, J.; Koo, G. C.; Koprak, S. L.; LeGrand, C. B.; Mundt, S. S.; Shah, K.; Springer, M. S.; Tan, E. Y.; Thieringer, R.; Hermanowski-Vosatka, A.; Zokian, H. J.; Balkovec, J.

- M.; Waddle, S. T. *Bioorg. Med. Chem. Lett.* **2005**, *15*, 5266; (e) Xiang, J.; Ipek, M.; Suri, V.; Masefski, W.; Pan, N.; Ge, Y.; Tam, M.; Xing, Y.; Tobin, J. F.; Xu, X.; Tam, S. *Bioorg. Med. Chem. Lett.* **2005**, *15*, 2865; (f) Coppola, G. M.; Kukkola, P. J.; Stanton, J. L.; Neubert, A. D.; Marcopulos, N.; Bilci, N. A.; Wang, H.; Tomaselli, H. C.; Tan, J.; Aicher, T. D.; Knorr, D. C.; Jeng, A. Y.; Dardik, B.; Chatelain, R. E. *J. Med. Chem.* **2005**, *48*, 6696.
2. For recent reviews, see: (a) Draper, N.; Stewart, P. M. *J. Endocrinol.* **2005**, *186*, 251; (b) Thieringer, R.; Hermannowski-Vosatka, A. *Expert Rev. Cardiovasc. Ther.* **2005**, *3*, 911; (c) Morton, N. M.; Paterson, J. M.; Masuzaki, H.; Holmes, M. C.; Staels, B.; Fievet, C.; Walker, B. R.; Flier, J. S.; Mullins, J. J.; Seckl, J. R. *Diabetes* **2004**, *53*, 931; (d) Tomlinson, J. W.; Walker, E. A.; Bujalska, I. J.; Draper, N.; Lavery, G. G.; Cooper, M. S.; Hewison, M.; Stewart, P. M. *Endocr. Rev.* **2004**, *25*, 831.
3. (a) Krozowski, Z.; Li, K. X. Z.; Koyama, K.; Smith, R. E.; Obeyesekere, V. R.; Stein-Oakley, A.; Sasano, H.; Coulter, C.; Cole, T.; Sheppard, K. E. *J. Steroid Biochem. Mol. Biol.* **1999**, *69*, 391; (b) Stewart, P. M.; Krozowski, Z. S.; Gupta, A.; Milford, D. V.; Howie, A. J.; Sheppard, M. C.; Whorwood, C. B. *Lacert* **1996**, *347*, 88; (c) Stewart, P. M. *J. Steroid Biochem. Mol. Biol.* **1999**, *69*, 403.
4. Patel, J. R.; Shuai, Q.; Link, J. T.; Rohde, J. J.; Dinges, J.; Sorensen, B. K.; Winn, M.; Yong, H.; Yeh, V. S. World Patent 074244, 2006, manuscript in preparation.
5. Freeman, F.; Chen, T.; van der Linden, J. B. *Synthesis* **1997**, 861.
6. (a) Zhang, H.; Cai, Q.; Ma, D. *J. Org. Chem.* **2005**, *70*, 5164; (b) Yeh, V. S. C.; Wiedeman, P. E. *Tetrahedron Lett.* **2006**, *47*, 6011.
7. Liu, X.; Hartwig, J. F. *J. Am. Chem. Soc.* **2004**, *126*, 5182.
8. The in vitro 11 $\beta$ -HSD-1 enzymatic assays are similar to the methods described in Ref.1a. Truncated human or mouse 11 $\beta$ -HSD-1, lacking the first 24 amino acids, was expressed in *Escherichia coli* using the pET28 expression system and the crude lysates were used as the enzyme source. The reaction was carried out with a total substrate (cortisone) concentration of 175 nM which contained 75 nM <sup>3</sup>H-cortisone and 181  $\mu$ M of the co-factor NADPH in 50 mM Tris-HCl, at pH 7.2 with 1 mM EDTA. The final enzyme concentration was 0.015 mg/mL to keep the substrate consumption rate below 25% at the end of the reaction. To ensure the reaction proceeds in the reductase direction, a NADPH regeneration system with 1 mM G-6-P and 1 U/mL G-6-PDH was included in the reaction. After incubating at room temperature for 30 min, the reaction was terminated by adding the non-selective 11 $\beta$ -HSD-1 inhibitor 18 $\beta$ -GA. The radioactive cortisol generated in the assay was captured by a monoclonal anti-cortisol antibody and SPA beads coated with anti-mouse antibodies. The plate was read using a Microbeta Liquid Scintillation Counter (Perkin-Elmer Life Sciences). The percent inhibition was calculated relative to a non-inhibited control and plotted against compound concentration to generate the IC<sub>50</sub> results. HEK assays: cellular activity of the compounds was evaluated in HEK293 cells which were stably transfected with full-length human 11 $\beta$ -HSD-1 cDNA. Cells were plated on poly-D lysine-coated plates (Becton-Dickinson Biocoat 35-4461) in DMEM containing 10% FBS, 300  $\mu$ g/mL geneticin, 100 U/mL penicillin, 100  $\mu$ g/mL streptomycin, and 0.25  $\mu$ g/mL Fungizone. The cells were pretreated with compounds for 30 min, followed by incubation with 1  $\mu$ M of substrate (cortisone) in dPBS buffer for 2 h at 37 °C in a 5% CO<sub>2</sub> atmosphere. The cell media were harvested and the cortisol concentration in the media was determined by fluorescence polarization immuno-assay (FPIA). A mixture of fluorescein-labeled cortisol and monoclonal anti-cortisol antibody was added to the well in the FPIA diluent buffer (Abbott Laboratories) to a final concentration 4 nM (cortisol) and 10 nM (mAb). The resulting fluorescent signal was read using an Analyst plate reader (LJL). The percent inhibition was calculated relative to a non-inhibited control and plotted against compound concentration to generate the IC<sub>50</sub> results.
9. Compounds were dissolved in 1% Tween 80 in 0.2% hydroxypropyl methylcellulose and administered to DIO mice as a single oral dose at 30 mpk. At 1, 7, and 16 h post-dose, fresh tissues including liver, epididymal fat pad (EFP), and brain were removed, immersed in PBS buffer, and weighed (3 mice per data point were used). The total volume of PBS buffer added was equivalent to approximately five times the mass of tissue. Tissues were minced into 2–3 mm pieces and the substrate (cortisone) was added to a final concentration of 10  $\mu$ M. The tissues were then incubated at 37 °C in a 5% CO<sub>2</sub> atmosphere for 20 min for liver and three hours for brain and adipose tissue. The cortisol concentration in the media was determined by LC-MS detection. The percent inhibition of 11 $\beta$ -HSD-1 activity was calculated relative to a vehicle control treated group. Ex vivo 11 $\beta$ -HSD-1 assays in *ob/ob* mice and other strains of rodents were conducted similarly.
10. Sandeep, T. C.; Yau, J. L.; MacLulich, A. M., et al. *Proc. Natl. Acad. Sci. U.S.A.* **2004**, *101*, 6734.